Measurements of branching fractions and *CP*-violating asymmetries in $B^0 \to \pi^+\pi^-$, $K^+\pi^-$, K^+K^- decays

Paul D. Dauncey (representing the BABAR Collaboration)
Blackett Laboratory
Imperial College
Prince Consort Road
London SW7 2BW, UK

1 Introduction

Recent measurements of the *CP*-violating asymmetry parameter $\sin 2\beta$ by the *BABAR* [1] and BELLE [2] collaborations established *CP* violation in the B^0 system. These measurements, as well as updated preliminary results [3, 4], are consistent with the Standard Model expectation based on measurements and theoretical estimates of the elements of the Cabibbo-Kobayashi-Maskawa [5] (CKM) quark-mixing matrix.

The study of B decays to charmless hadronic two-body final states will yield important information about the remaining angles (α and γ) of the Unitarity Triangle. In the Standard Model, the time-dependent *CP*-violating asymmetry in the decay $B^0 \to \pi^+\pi^-$ is related to the angle α, nd ratios of branching fractions for various $\pi\pi$ and $K\pi$ decay modes are sensitive to the angle γ. We previously reported measurements of branching fractions [6] and *CP*-violating asymmetries [7] n $B^0 \to \pi^+\pi^-$, $K^+\pi^-$, and K^+K^- decays. (Unless explicitly stated, charge conjugate decay modes are assumed throughout this paper.) In this paper, we present a preliminary update of these results using a sample of 60 million $B\overline{B}$ pairs.

We reconstruct a sample of B mesons ($B_{\rm rec}$) decaying to the $h^+h'^-$ final state, where h and h' refer to π or K, and examine the remaining charged particles in each event to "tag" the flavor of the other B meson ($B_{\rm tag}$). The decay rate distribution f_+ (f_-) when $h^+h'^- = \pi^+\pi^-$ and $B_{\rm tag} = B^0$ ($\overline{B}^0$) is given by

$$f_\pm(\Delta t) = \frac{e^{-|\Delta t|/\tau}}{4\tau}\left[1 \pm S_{\pi\pi}\sin(\Delta m_d \Delta t) \mp C_{\pi\pi}\cos(\Delta m_d \Delta t)\right], \tag{1}$$

where τ is the mean B^0 lifetime, Δm_d is the eigenstate mass difference, and $\Delta t = t_{\rm rec} - t_{\rm tag}$ is the time between the $B_{\rm rec}$ and $B_{\rm tag}$ decays. The *CP*-violating parameters $S_{\pi\pi}$ and $C_{\pi\pi}$ are defined in terms of a complex parameter λ as

$$S_{\pi\pi} = \frac{2\,\mathcal{I}m\lambda}{1+|\lambda|^2} \qquad \text{and} \qquad C_{\pi\pi} = \frac{1-|\lambda|^2}{1+|\lambda|^2}. \tag{2}$$

If the decay proceeds purely through the $b \to uW^-$ tree process, then λ is given in terms of the CKM elements $V_{\rm ij}$ by

$$\lambda(B \to \pi^+\pi^-) = \left(\frac{V^*_{\rm tb}V_{\rm td}}{V_{\rm tb}V^*_{\rm td}}\right)\left(\frac{V^*_{\rm ud}V_{\rm ub}}{V_{\rm ud}V^*_{\rm ub}}\right). \tag{3}$$

In this case, $C_{\pi\pi} = 0$ and $S_{\pi\pi} = \sin 2\alpha$, where $\alpha \equiv \arg\left[-V_{\rm td}V^*_{\rm tb}/V_{\rm ud}V^*_{\rm ub}\right]$. In general, the $b \to dg$ penguin amplitude modifies both the magnitude and phase of λ, so that $C_{\pi\pi} \neq 0$ and $S_{\pi\pi} = \sqrt{1 - C^2_{\pi\pi}}\sin 2\alpha_{\rm eff}$, where $\alpha_{\rm eff}$ depends on the magnitudes and relative strong and weak phases of the tree and penguin amplitudes. Several approaches have been proposed to obtain information on α in the presence of penguins [8].

2 The *BABAR* detector and dataset

The data sample used in this analysis consists of 55.6 fb^{-1}, corresponding to 60.2 ± 0.7 million $B\overline{B}$ pairs, collected on the $\Upsilon(4S)$ resonance with the *BABAR* detector at the SLAC PEP-II storage ring between October 1999 and December 2001. Equal branching fractions for $\Upsilon(4S) \to B^0\overline{B}^0$ and B^+B^- are assumed.

A detailed description of the *BABAR* detector is presented in [9]. Charged particle (track) momenta are measured in a tracking system consisting of a 5-layer double-sided silicon vertex tracker (SVT) and a 40-layer drift chamber (DCH) filled with a gas mixture of helium and isobutane. The SVT and DCH operate within a 1.5 T superconducting solenoidal magnet. Photons are detected in an electromagnetic calorimeter (EMC) consisting of 6580 CsI(Tl) crystals arranged in barrel and forward endcap subdetectors. The flux return for the solenoid is composed of multiple layers of iron and resistive plate chambers for the identification of muons and long-lived neutral hadrons. Tracks from the $B_{\rm rec}$ decay are identified as pions or kaons by the Cherenkov angle θ_c measured with a detector of internally reflected Cherenkov light (DIRC).

3 Analysis method

Event selection is identical to that described in [7]. Candidate $B_{\rm rec}$ decays are reconstructed from pairs of oppositely-charged tracks forming a good quality vertex, where the $B_{\rm rec}$ four-vector is calculated assuming the pion mass for both tracks. We require each track to have an associated θ_c measurement with a minimum of six Cherenkov photons above background, where the average is approximately 30 for both pions and kaons. Protons are rejected based on θ_c and electrons are rejected based on dE/dx measurements in the tracking system, shower shape in the EMC, and the ratio of shower energy and track momentum. Background from the reaction $e^+e^- \to q\overline{q}$ ($q = u, d, s, c$) is suppressed by removing jet-like events from the sample:

we define the center-of-mass (CM) angle θ_S between the sphericity axes of the B candidate and the remaining tracks and photons in the event, and require $|\cos\theta_S| < 0.8$, which removes 83% of the background. The total efficiency for signal events of the above selection is approximately 38%.

Signal decays are identified kinematically using two variables. We define a beam-energy substituted mass $m_{\rm ES} = \sqrt{E_{\rm b}^2 - \mathbf{p}_B^2}$, where the B candidate energy is defined as $E_{\rm b} = (s/2 + \mathbf{p}_i \cdot \mathbf{p}_B)/E_i$, $\sqrt{s}$ and E_i are the total energies of the e^+e^- system in the CM and laboratory frames, respectively, and $\mathbf{p}_i$ and $\mathbf{p}_B$ are the momentum vectors in the laboratory frame of the e^+e^- system and the $B_{\rm rec}$ candidate, respectively. Signal events are Gaussian distributed in $m_{\rm ES}$ with a mean near the B mass and a resolution of $2.6\,{\rm MeV}/c^2$, dominated by the beam energy spread. The background shape is parameterized by a threshold function [10] with a fixed endpoint given by the average beam energy.

We define a second kinematic variable ΔE as the difference between the energy of the $B_{\rm rec}$ candidate in the CM frame and $\sqrt{s}/2$. Signal $\pi\pi$ decays are Gaussian distributed with a mean value near zero. For decays with one (two) kaons, the distribution is shifted relative to $\pi\pi$ on average by $-45\,{\rm MeV}$ ($-91\,{\rm MeV}$), respectively, where the exact separation depends on the laboratory momentum of the kaon(s). The resolution on ΔE is approximately 26 MeV and is validated in large samples of fully reconstructed B decays. The background is parameterized by a quadratic function.

Candidate $h^+h'^-$ pairs selected in the region $5.2 < m_{\rm ES} < 5.3\,{\rm GeV}/c^2$ and $|\Delta E| < 0.15\,{\rm GeV}$ are used to extract yields and *CP*-violating asymmetries with an unbinned maximum likelihood fit. The total number of events in the fit region satisfying all of the above criteria is 17585.

To determine the flavor of the $B_{\rm tag}$ meson we use the same B-tagging algorithm used in the *BABAR* $\sin 2\beta$ analysis [11]. The algorithm relies on the correlation between the flavor of the b quark and the charge of the remaining tracks in the event after removal of the $B_{\rm rec}$ candidate. We define five mutually exclusive tagging categories: `Lepton`, `Kaon`, `NT1`, `NT2`, and `Untagged`. `Lepton` tags rely on primary electrons and muons from semileptonic B decays, while `Kaon` tags exploit the correlation in the process $b \to c \to s$ between the net kaon charge and the charge of the b quark. The `NT1` (more certain tags) and `NT2` (less certain tags) categories are derived from a neural network that is sensitive to charge correlations between the parent B and unidentified leptons and kaons, soft pions, or the charge and momentum of the track with the highest CM momentum. The addition of `Untagged` events improves the signal yield estimates and provides a larger sample for determining background shape parameters directly in the maximum likelihood fit.

The quality of tagging is expressed in terms of the effective efficiency $Q = \sum_c \epsilon_c D_c^2$, where ϵ_c is the fraction of events tagged in category c and the dilution $D_c = 1 - 2w_c$ is related to the mistag fraction w_c. Table 1 summarizes the tagging performance in a data sample $B_{\rm flav}$ of fully reconstructed neutral B decays into $D^{(*)-}h^+$ ($h^+ =$

Category	ϵ (%)	D (%)	ΔD (%)	Q (%)
`Lepton`	11.1 ± 0.2	82.8 ± 1.8	-1.2 ± 3.0	7.6 ± 0.4
`Kaon`	34.7 ± 0.4	63.8 ± 1.4	1.8 ± 2.1	14.1 ± 0.6
`NT1`	7.6 ± 0.2	56.0 ± 3.0	-2.7 ± 4.7	2.4 ± 0.3
`NT2`	14.0 ± 0.3	25.4 ± 2.6	9.4 ± 3.8	0.9 ± 0.2
`Untagged`	32.6 ± 0.5	–	–	–
Total Q				25.0 ± 0.8

Table 1: Tagging efficiency ϵ, average dilution $D = 1/2\,(D_{B^0} + D_{\overline{B}^0})$, dilution difference $\Delta D = D_{B^0} - D_{\overline{B}^0}$, and effective tagging efficiency Q for signal events in each tagging category. The values are measured in the $B_{\rm flav}$ sample.

π^+, ρ^+, a_1^+) and $J/\psi\, K^{*0}$ ($K^{*0} \to K^+\pi^-$) flavor eigenstates. We use the same tagging efficiencies and dilutions for signal $\pi\pi$, $K\pi$, and KK decays. Separate background efficiencies for each species are determined simultaneously with $S_{\pi\pi}$ and $C_{\pi\pi}$ in the maximum likelihood fit.

The time difference Δt is obtained from the measured distance between the z positions of the $B_{\rm rec}$ and $B_{\rm tag}$ decay vertices and the known boost of the e^+e^- system. The z position of the $B_{\rm tag}$ vertex is determined with an iterative procedure that removes tracks with a large contribution to the total χ^2. An additional constraint is constructed from the three-momentum and vertex position of the $B_{\rm rec}$ candidate, and the average e^+e^- interaction point and boost. For 99.5% of candidates with a reconstructed vertex, the rms Δz resolution is $180\,\mu$m (1.1 ps). We require $|\Delta t| < 20$ ps and $\sigma_{\Delta t} < 2.5$ ps, where $\sigma_{\Delta t}$ is the error on Δt. The resolution function for signal candidates is a sum of three Gaussians, identical to the one described in [3], with parameters determined from a fit to the $B_{\rm flav}$ sample (including events in all five tagging categories). The background Δt distribution is parameterized as the sum of an exponential convolved with a Gaussian, and two additional Gaussians to account for tails. A common parameterization is used for all tagging categories, and the parameters are determined simultaneously with the *CP* parameters in the maximum likelihood fit. We find that 86% of background events are described by an effective lifetime of about 0.6 ps, while tails are described by 12 (2)% of events with a resolution of approximately 2 (8) ps.

Discrimination of signal from light-quark background is enhanced by the use of a Fisher discriminant $\mathcal{F}$ [6]. The discriminating variables are constructed from the scalar sum of the CM momenta of all tracks and photons (excluding tracks from the $B_{\rm rec}$ candidate) entering nine two-sided 10-degree concentric cones centered on the thrust axis of the $B_{\rm rec}$ candidate. The distribution of $\mathcal{F}$ for signal events is parameterized as a single Gaussian, with parameters determined from Monte Carlo simulated decays and validated with $B^- \to D^0\pi^-$ decays reconstructed in data. The

background shape is parameterized as the sum of two Gaussians, with parameters determined directly in the maximum likelihood fit.

Identification of $h^+h'^-$ tracks as pions or kaons is accomplished with the Cherenkov angle measurement from the DIRC. We construct Gaussian probability density functions (PDFs) from the difference between measured and expected values of θ_c for the pion or kaon hypothesis, normalized by the resolution. The DIRC performance is parameterized using a sample of $D^{*+} \to D^0\pi^+$, $D^0 \to K^-\pi^+$ decays, reconstructed in data. Figure 1 shows the typical separation between pions and kaons, which varies from 8σ at momenta of 2 GeV/c to 2.5σ at 4 GeV/c, where σ is the average resolution of θ_c.

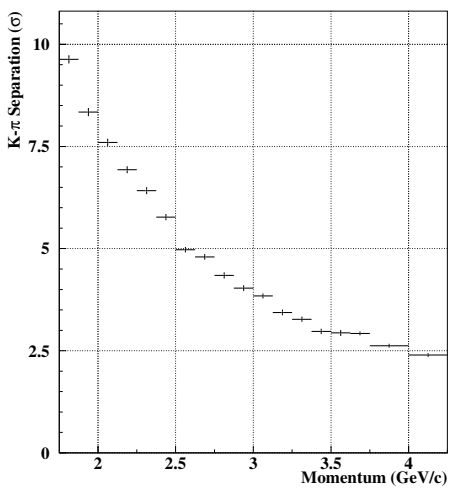

Figure 1: Variation of the separation between the kaon and pion Cherenkov angles with momentum, as obtained from a control sample of $D^{*+} \to D^0\pi^+$, $D^0 \to K^-\pi^+$ decays reconstructed in data.

4 Results

We use unbinned extended maximum likelihood fits to extract yields and *CP* parameters from the $B_{\rm rec}$ sample. The likelihood for candidate j tagged in category c is obtained by summing the product of event yield n_i, tagging efficiency $\epsilon_{i,c}$, and probability $\mathcal{P}_{i,c}$ over the eight possible signal and background hypotheses i (referring to $\pi\pi$, $K^+\pi^-$, $K^-\pi^+$, and KK decays),

$$\mathcal{L}_c = \exp\left(-\sum_i n_i\epsilon_{i,c}\right)\prod_j\left[\sum_i n_i\epsilon_{i,c}\mathcal{P}_{i,c}(\vec{x}_j;\vec{\alpha}_i)\right]. \tag{4}$$

Mode	ϵ_T (%)	N_S (Events)	$\mathcal{B}$ (10^{-6})
$\pi^+\pi^-$	38.5 ± 0.7	$124^{+16\,+7}_{-15\,-9}$	$5.4 \pm 0.7 \pm 0.4$
$K^+\pi^-$	37.6 ± 0.7	$403 \pm 24 \pm 15$	$17.8 \pm 1.1 \pm 0.8$
K^+K^-	36.7 ± 0.7	< 16 (90% C.L.)	< 1.1 (90% C.L.)

Table 2: Summary of results for total detection efficiencies ϵ_T, fitted signal yields N_S and measured branching fractions $\mathcal{B}$.

For the $K^\mp\pi^\pm$ components, the yield is parameterized as $n_i = N_{K\pi}\left(1 \pm \mathcal{A}_{K\pi}\right)/2$, where $N_{K\pi} = N_{K^-\pi^+} + N_{K^+\pi^-}$ and $\mathcal{A}_{K\pi} \equiv (N_{K^-\pi^+} - N_{K^+\pi^-})/(N_{K^-\pi^+} + N_{K^+\pi^-})$. The probabilities $\mathcal{P}_{i,c}$ are evaluated as the product of PDFs for each of the independent variables $\vec{x}_j = \{m_{\rm ES}, \Delta E, \mathcal{F}, \theta_c^+, \theta_c^-, \Delta t\}$, where θ_c^+ and θ_c^- are the Cherenkov angles for the positively and negatively charged tracks. We use identical PDFs for θ_c^+ and θ_c^-. The total likelihood $\mathcal{L}$ is the product of likelihoods for each tagging category and the free parameters are determined by minimizing the quantity $-\ln\mathcal{L}$.

4.1 Time-independent fit

In order to minimize the systematic error on the branching fraction measurements, we perform an initial fit without tagging or Δt information. A total of 16 parameters are varied in the fit, including signal and background yields (6 parameters) and asymmetries (2), and parameters for the background shapes in $m_{\rm ES}$ (1), ΔE (2), and $\mathcal{F}$ (5).

Table 2 summarizes results for total efficiencies, signal yields and branching fractions. The upper limit on the signal yield for $B^0 \to K^+K^-$ is given by the value of n^0 for which $\int_0^{n^0} \mathcal{L}_{\rm max}\, dn / \int_0^\infty \mathcal{L}_{\rm max}\, dn = 0.90$, where $\mathcal{L}_{\rm max}$ is the likelihood as a function of n, maximized with respect to the remaining fit parameters. The branching fraction upper limit is calculated by increasing the signal yield upper limit and reducing the efficiency by their respective systematic errors. The fit result for the $K\pi$ charge asymmetry $\mathcal{A}_{K\pi}$ is

$$\mathcal{A}_{K\pi} = -0.05 \pm 0.06 \pm 0.01, \qquad 90\%\ \text{C.L.}\ -0.14 < \mathcal{A}_{K\pi} < 0.05. \tag{5}$$

The statistical and systematic errors on $\mathcal{A}_{K\pi}$ are added in quadrature when calculating the 90% confidence level (C.L.).

The dominant systematic error on the branching fraction measurements is due to uncertainty in the shape of the θ_c PDF, while the dominant error on $\mathcal{A}_{K\pi}$ is due to possible charge bias in track and θ_c reconstruction. All measurements are consistent with our previous results reported in [6].

Figure 2 shows distributions of $m_{\rm ES}$ and ΔE after a cut on likelihood ratios. We define $\mathcal{R}_{\rm sig} = \sum_s n_s\mathcal{P}_s / \sum_i n_i\mathcal{P}_i$ and $\mathcal{R}_k = n_k\mathcal{P}_k / \sum_s n_s\mathcal{P}_s$, where $\sum_s\,(\sum_i)$ indicates

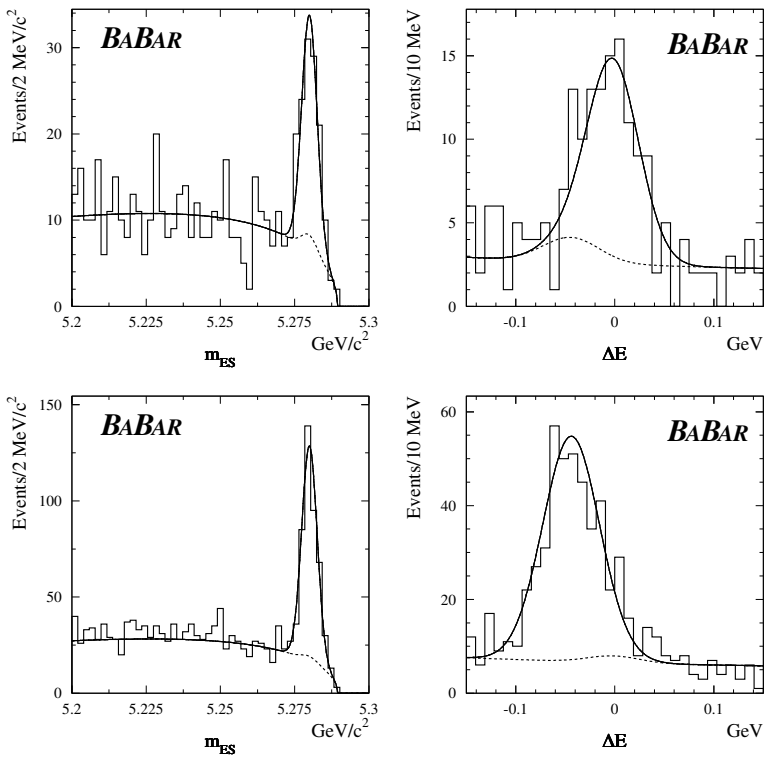

Figure 2: Distributions of $m_{\rm ES}$ (left) and ΔE (right) for events enhanced in signal $\pi\pi$ (top) and $K\pi$ (bottom) decays based on the likelihood ratio selection described in the text. Solid curves represent projections of the maximum likelihood fit result after accounting for the efficiency of the additional selection, while dashed curves represent $q\overline{q}$ and $\pi\pi \leftrightarrow K\pi$ cross-feed background.

a sum over signal (all) hypotheses, and $\mathcal{P}_k$ indicates the probability for signal hypothesis k. The probabilities include the PDFs for θ_c, $\mathcal{F}$, and $m_{\rm ES}$ (ΔE) when plotting ΔE ($m_{\rm ES}$). The selection is defined by optimizing the signal significance with respect to $\mathcal{R}_{\rm sig}$ and $\mathcal{R}_k$. The solid curve in each plot represents the fit projection after correcting for the efficiency of the additional selection (approximately 67% for $\pi\pi$ and 88% for $K\pi$).

4.2 Time-dependent fit

The time-dependent *CP* asymmetries $S_{\pi\pi}$ and $C_{\pi\pi}$ are determined from a second fit including tagging and Δt information, with the yields and $\mathcal{A}_{K\pi}$ fixed to the results of the first fit. The Δt PDF for signal $\pi^+\pi^-$ decays is given by Eq. (1), modified to include the dilution and dilution difference for each tagging category, and convolved

with the signal resolution function. The Δt PDF for signal $K\pi$ events takes into account B^0–$\overline{B}^0$ mixing, depending on the charge of the kaon and the flavor of $B_{\rm tag}$. We parameterize the Δt distribution in $B^0 \to K^+K^-$ decays as an exponential convolved with the resolution function.

A total of 34 parameters are varied in the fit, including the values of $S_{\pi\pi}$ and $C_{\pi\pi}$, separate background tagging efficiencies for $\pi\pi$, $K\pi$, and KK events (12), parameters for the background Δt resolution function (8), and parameters for the background shapes in $m_{\rm ES}$ (5), ΔE (2), and $\mathcal{F}$ (5). The signal tagging efficiencies and dilutions are fixed to the values in Table 1, while τ and Δm_d are fixed to their PDG values [12]. For each parameter, we also calculate the 90% C.L. interval taking into account the systematic error. The fit yields

$$\begin{aligned} S_{\pi\pi} &= -0.01 \pm 0.37 \pm 0.07, \qquad 90\%\ \text{C.L.}\ -0.66 < S_{\pi\pi} < 0.62, \\ C_{\pi\pi} &= -0.02 \pm 0.29 \pm 0.07, \qquad 90\%\ \text{C.L.}\ -0.54 < C_{\pi\pi} < 0.48, \end{aligned} \tag{6}$$

and the correlation between $S_{\pi\pi}$ and $C_{\pi\pi}$ is -13%.

Systematic uncertainties on $S_{\pi\pi}$ and $C_{\pi\pi}$ are dominated by the uncertainty on the shape of the θ_c PDF. Since we measure asymmetries near zero, multiplicative systematic errors have also been evaluated (0.05). We sum in quadrature multiplicative errors, evaluated at one standard deviation, with the additive systematic uncertainties.

To validate the analysis technique, we measure τ and Δm_d in the $B_{\rm rec}$ sample and find $\tau = (1.66 \pm 0.09)\,\text{ps}$ and $\Delta m_d = (0.517 \pm 0.062)\hbar\,\text{ps}^{-1}$. Figure 3 shows the asymmetry $\mathcal{A}_{\rm mix} = (N_{\rm unmixed} - N_{\rm mixed})/(N_{\rm unmixed} + N_{\rm mixed})$ in a sample of events enhanced in $B \to K\pi$ decays. The curve shows the expected oscillation given the value of Δm_d measured in the full sample.

For tagged events enhanced in signal $\pi\pi$ decays, Figure 4 shows the Δt distributions and the asymmetry $\mathcal{A}_{\pi\pi}(\Delta t) = [N_{B^0}(\Delta t) - N_{\overline{B}^0}(\Delta t)]/[N_{B^0}(\Delta t) + N_{\overline{B}^0}(\Delta t)]$. The selection procedure is the same as for Figure 2, with the likelihoods defined including the PDFs for θ_c, $\mathcal{F}$, $m_{\rm ES}$, and ΔE.

5 Summary

In summary, we have presented updated preliminary measurements of branching fractions and *CP*-violating asymmetries in $B^0 \to \pi^+\pi^-$, $K^+\pi^-$, and K^+K^- decays. All results are consistent with our previous measurements. No evidence for *CP* violation is observed and our measurement of $\mathcal{A}_{K\pi}$ disfavors theoretical models that predict a large asymmetry [13, 14].

We are grateful for the extraordinary contributions of our PEP-II colleagues in achieving the excellent luminosity and machine conditions that have made this work possible.

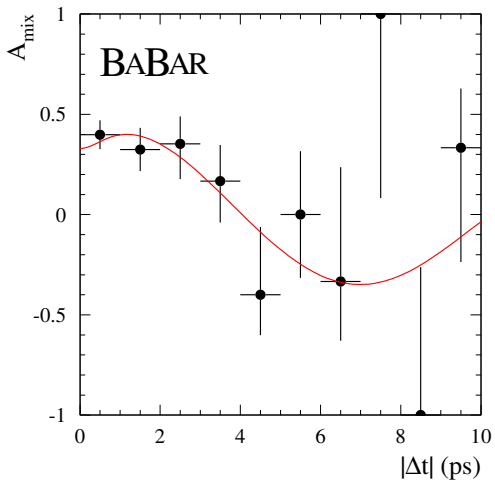

Figure 3: The asymmetry $\mathcal{A}_{\rm mix}$ between unmixed and mixed events in a sample enhanced in $K\pi$ decays. The curve indicates the expected oscillation corresponding to $\Delta m_d = 0.517\,\hbar\,{\rm ps}^{-1}$. The dilution from $q\overline{q}$ events is evident in the reduced amplitude near $|\Delta t| = 0$.

References

[1] *BABAR* Collaboration, B. Aubert *et al.*, Phys. Rev. Lett. **87**, 091801 (2001).

[2] BELLE Collaboration, K. Abe *et al.*, Phys. Rev. Lett. **87**, 091802 (2001).

[3] *BABAR* Collaboration, B. Aubert *et al.*, hep-ex/0203007 (2002).

[4] BELLE Collaboration, T. Higuchi, hep-ex/0205020 (2002).

[5] N. Cabibbo, Phys. Rev. Lett. **10**, 531 (1963); M. Kobayashi and T. Maskawa, Prog. Th. Phys. **49**, 652 (1973).

[6] *BABAR* Collaboration, B. Aubert *et al.*, Phys. Rev. Lett. **87**, 151802 (2001).

[7] *BABAR* Collaboration, B. Aubert *et al.*, Phys. Rev. D **65**, 051502 (2002).

[8] M. Gronau and D. London, Phys. Rev. Lett. **65**, 3381 (1990); Y. Grossman and H.R. Quinn, Phys. Rev. D **58**, 017504 (1998); J. Charles, Phys. Rev. D **59**, 054007 (1999); M. Gronau, D. London, N. Sinha, and R. Sinha, Phys. Lett. B **514**, 315 (2001); M. Beneke, G. Buchalla, M. Neubert, and C.T. Sachrajda, Nucl. Phys. B **606**, 245 (2001).

[9] *BABAR* Collaboration, B. Aubert *et al.*, Nucl. Instr. and Methods A **479**, 1 (2002).

[10] ARGUS Collaboration, H. Albrecht *et al.*, Z. Phys. C **48**, 543 (1990).

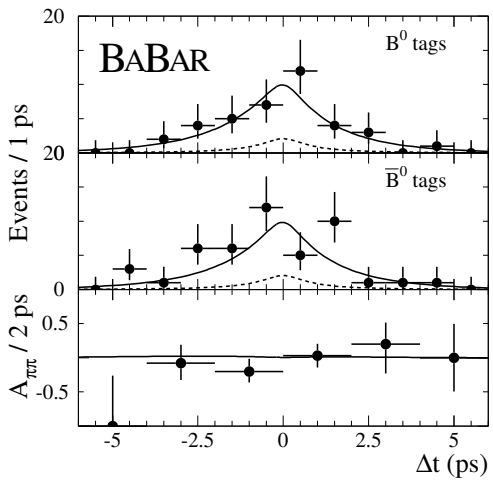

Figure 4: Distributions of Δt for events enhanced in signal $\pi\pi$ decays based on the likelihood ratio selection described in the text. The top two plots show events (points with errors) with $B_{\rm tag} = B^0$ or $\overline{B}^0$. Solid curves represent projections of the maximum likelihood fit, dashed curves represent the sum of $q\overline{q}$ and $K\pi$ background events. The bottom plot shows $\mathcal{A}_{\pi\pi}(\Delta t)$ for data (points with errors) and the fit projection.

[11] *BABAR* Collaboration, B. Aubert *et al.*, hep-ex/0201020, accepted by Phys. Rev. D.

[12] Particle Data Group, D.E. Groom *et al.*, Eur. Phys. Jour. C **15**, 1 (2000).

[13] Y.Y. Keum, H-n. Li, and A.I. Sanda, Phys. Rev. D **63**, 054008 (2001).

[14] M. Ciuchini *et al.*, Phys. Lett. B **515**, 33 (2001).